Steel and Composite Structures, *Vol. 25, No. 2 (2017) 127-139*
DOI: https://doi.org/10.12989/scs.2017.25.2.127

Analytical solutions for sandwich plates considering permeation effect by 3-D elasticity theory

Ruili Huo, Weiqing Liu, Peng Wu and Ding Zhou*

College of Civil Engineering, Nanjing Tech University, 211800 Nanjing, China

(*Received March 14, 2017, Revised June 12, 2017, Accepted June 17, 2017*)

Abstract. In this paper, an exact analytical solution for simply supported sandwich plate which considers the permeation effect of adhesives is presented. The permeation layer is described as functionally graded material (FGM), the elastic modulus of which is assumed to be graded along the thickness following the exponential law. Based on the exact three-dimensional (3-D) elasticity theory, the solution of stresses and displacements for each layer is derived. By means of the recursive matrix method, the solution can be efficiently obtained for plates with many layers. The present solution obtained can be used as a benchmark to access other simplified solutions. The comparison study indicates that the finite element (FE) solution is close to the present one when the FGM layer in the FE model is divided into a series of homogeneous layers. However, the present method is more efficient than the FE method, with which the mesh division and computation are time-consuming. Moreover, the solution based on Kirchhoff-Love plate theory is greatly different from the present solution for thick plates. The influence of the thickness of the permeation layer on the stress and displacement fields of the sandwich plate is discussed in detail. It is indicated that the permeation layer can effectively relieve the discontinuity stress at the interface.

Keywords: sandwich plate; permeation effect; functionally graded material; elasticity solution; recursive matrix method

1. Introduction

Thanks to the advantages of high strength, high stiffness, low density, anti-fatigue and corrosion resistance, composite structures are increasingly used in civil, mechanical and aeronautical engineering. Additionally, the mechanical property of composite structures can be tailored by changing material type and the compose pattern. The sandwich plate (Iivani *et al*. 2016, Yan and Song 2016, Arani *et al*. 2016, Huang and Liew 2016, Nguyen *et al*. 2016 and Qu *et al*. 2016) is a typical application, which consists of face, core and adhesive layers, as shown in Fig. 1.

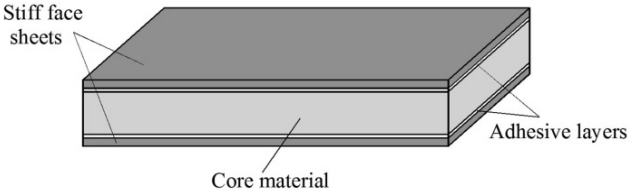

Fig. 1 Components schematic of sandwich structure

However, in practice the adhesive will permeate into the core and face layers, as shown in Fig. 2. The permeation layer is the mixture of face (or core) layer and the adhesive. It is widely known that the interfacial damage and debonding of sandwich structures often occurs because of the large discontinuity stress at the interface. The permeation layer makes the material property of the sandwich plate continuously vary along the thickness, which is similar to FGM. The continuous material distributions are good to reduce discontinuity stress at the interface. Such a problem deserves to be deeply investigated.

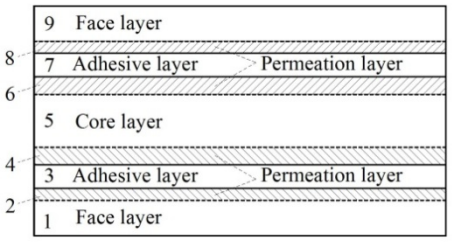

Fig. 2 Permeation effect of adhesives

The simplified plate theories, such as the Kirchhoff plate theory, the Mindlin plate theory and the higher-order shear deformation theory, are widely used to study the mechanical behaviors of FGM plates. Mantari and Monge (2016) developed an analytical solution to study the buckling, free vibration and bending behaviors of simply supported FGM sandwich plates subjected to transverse and axial mechanical loads. By using the nonlocal hyperbolic refined model, Belkorissat *et al*. (2015) studied the free vibration property of FGM plates. Li *et al*. (2016) proposed a four-variable refined plate theory to analyze the thermo-mechanical bending of FGM sandwich plates. The face and core layers were both modeled by FGM. Bouchafa *et al*. (2015) proposed a novel refined hyperbolic shear deformation theory, which involves only four unknown functions, to analyze the thermoelastic bending behavior of

*Corresponding author, Professor,
E-mail: dingzhou57@yahoo.com

ISSN: 1229-9367 (Print), 1598-6233 (Online)

FGM sandwich plates. The buckling problem of FGM plates subjected to thermal and mechanical loads was analyzed by Yu *et al*. (2017). The deformation of the plate is represented by the Mindlin plate theory. Based on the higher-order shear deformation theory, the bending, vibration and buckling behaviors of FGM sandwich plates were investigated by Nguyen *et al*. (2015a). The dynamic response of FGM steel composite cylindrical panels in steady-state thermal environments subjected to impulsive loads was firstly investigated by Isavand *et al*. (2015). By means of the discrete singular convolution method, Civalek (2017) investigated the free vibration of annular plates made of composite FGM based on Mindlin plate theory. By using the Laplace transformation method, Li *et al*. (2014) studied the time-dependent behavior of two-layer FGM structures sandwiching a thin viscoelastic interlayer. A refined shear deformation theory was proposed by Thai and Uy (2013) to analyze the buckling behavior of FGM plate. The position of neutral surface is determined and the governing stability equations were obtained. Tebboune *et al*. (2015) presented a trigonometric shear deformation theory for thermal buckling analysis of FGM plates. This theory accounted for sinusoidal distribution of transverse shear stress without using the shear correction factor. Based on the non-polynomial higher order shear deformation theory, Mantari *et al*. (2014) investigated the free vibration of functionally graded plates resting on elastic foundation. Yarasca *et al*. (2016) presented the static analysis for functionally graded sandwich structures by using the 7DOFs quasi-3D hybrid element. Viola *et al*. (2012) presented an unconstrained third-order shear deformation theory to evaluate the tangential and normal stresses in moderately thick functionally graded cylindrical panels.

Besides the classical plate theory and higher-order theories, some numerical methods presented recently are efficient for analysis of FGM plates. Based on the isogeometric approach, the static, dynamic and buckling behaviors of FGM plates were studied by Thai *et al*. (2014a) and Nguyen *et al*. (2015b). The main advantages of the isogeometric approach are the ability to exactly represent domains with conic sections and can achieve better approximation with arbitrarily high smoothness. By means of the meshfree method, the static and dynamic problems for layered FGM plates were investigated by Vu *et al*. (2017) and Bui *et al*. (2011, 2013). In the meshfree method, the domain of mechanic problems is discretized by scattered nodes and no elements are required. Bui *et al*. (2016) presented a displacement-based finite element formulation associated with a novel third-order shear deformation plate theory to analyze the bending and natural frequencies of functionally graded plates under high temperature field. Based on the isogeometric analysis and the quasi-3D hyperbolic shear deformation theory, Liu *et al*. (2017) studied the bending, free vibration and buckling behaviors of functionally graded plates. Five unknowns per node are included, and the shear locking phenomenon is avoided. Thai *et al*. (2014b) developed a quasi-3D hyperbolic shear deformation theory for functionally graded plates. Both shear deformation and thickness stretching effects were considered.

The 3-D elasticity theory is always recognized as benchmark to access other simplified solution (Chen and Lee 2004). Pagano (1969, 1970) presented analytical solutions for laminate plates composed of arbitrary numbers of layers. Using p-Ritz method, Wang *et al*. (2000) tackled free vibration for skew sandwich plates composed of two laminated facings sandwiching an orthotropic core. Based on the 3-D elasticity theory, Zenkour (2007) presented analytical solutions with high accuracy for single-layer FGM plates subjected to transverse load. The stress and displacement components were derived by using the state space method which greatly simplifies the analytical process.

In this study, based on the exact 3-D elasticity theory, a refined sandwich plate model which considers the permeation effect of adhesives is developed. The permeation layer is described as FGM, which is exponentially graded along the thickness. Unlike the single-layer FGM plate from Zenkour (2007), the present multilayer plate is composed of alternate fully homogeneous layers and FGM layers which follow a simple exponential law same as that used by Zenkour (2007). A typical example is the laminate glued by the macrovoid materials such as balsa wood. By means of the recursive matrix method, the solution of stresses and displacements can be efficiently obtained for the plate with many layers. The influence of the thickness of the permeation layer on the stresses and displacements of the plate is discussed in detail.

2. Elasticity solution for the sandwich plate model

2.1 Basic equations

Without loss of generality, we consider a sandwich plate with length a, width b and thickness H, consisting of alternate fully homogeneous layers and FGM with each thickness h_i, as shown in Fig. 3. The plate is subjected to normal load $q(x, y)$ acting on the top surface and is simply supported at four edges. Two Cartesian coordinate systems are established: the global coordinate system O-xyz with origin O at the bottom of the plate and the local coordinate system O_i-xyz_i with origin O_i at the bottom of the ith layer.

The permeation layer is a mixture one made of face (or core) layer material and the adhesive material. It is difficult to explicitly describe its mechanical properties unless the experimental measurement is carried out. Here, we assume the material property of the permeation layer is graded along the thickness following the exponential law, i.e., $E_i(z_i) = E_0^i e^{k_i z_i}$, where E_0^i denotes the elastic modulus at the lower surface of the ith layer and k_i denotes the gradient index for the ith layer. This model has two features: (1) the parameters used to describe the mixture layer is the fewest. Only the thickness of the layer and the elasticity moduli at the lower and upper surfaces of the layer is needed. (2) A fully homogeneous layer can also include in the model by letting $k_i = 0$ only. The elastic modulus at the upper and lower surfaces of the permeation layers are continuous, i.e., $E_i(h_i) = E_{i+1}$ and $E_i(0) = E_{i-1}$. The Poisson's ratio μ_i is

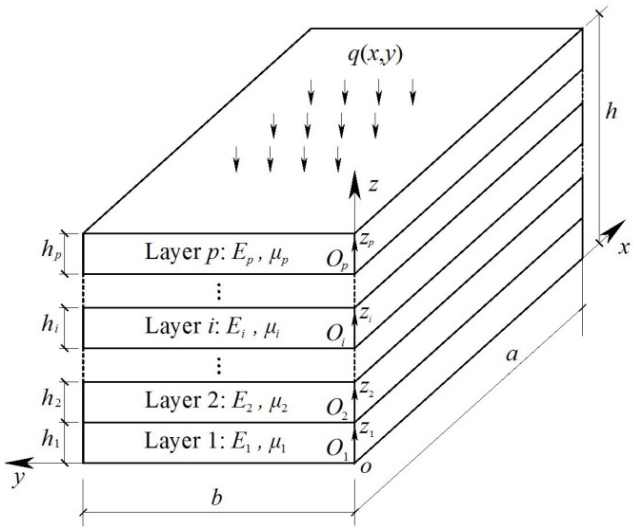

Fig. 3 Geometric shape and Cartesian coordinates of the sandwich plate

assumed to be constant in each layer.

Consider the *i*th (i = 1, 2…p) layer within the local coordinate system O_i-xyz_i. According to the 3-D elasticity theory, the constitutive relations are given by

$$\begin{aligned}
\sigma_x^i &= (\lambda^i + 2G^i)\frac{\partial u^i}{\partial x} + \lambda^i \frac{\partial v^i}{\partial y} + \lambda^i \frac{\partial w^i}{\partial z_i},\\
\sigma_y^i &= (\lambda^i + 2G^i)\frac{\partial v^i}{\partial y} + \lambda^i \frac{\partial u^i}{\partial x} + \lambda^i \frac{\partial w^i}{\partial z_i},\\
\sigma_{z_i}^i &= (\lambda^i + 2G^i)\frac{\partial w^i}{\partial z_i} + \lambda^i \frac{\partial u^i}{\partial x} + \lambda^i \frac{\partial v^i}{\partial y},\\
\tau_{yz_i}^i &= G^i\left(\frac{\partial v^i}{\partial z_i} + \frac{\partial w^i}{\partial y}\right), \quad \tau_{xz_i}^i = G^i\left(\frac{\partial u^i}{\partial z_i} + \frac{\partial w^i}{\partial x}\right),\\
\tau_{xy}^i &= G^i\left(\frac{\partial u^i}{\partial y} + \frac{\partial v^i}{\partial x}\right),
\end{aligned} \tag{1}$$

where σ_x^i, σ_y^i, $\sigma_{z_i}^i$, $\tau_{yz_i}^i$, $\tau_{xz_i}^i$ and τ_{xy}^i denote the stress components; u^i, v^i and w^i denote the displacement components in x, y and z directions, respectively; λ^i and G^i are the Lame constants, defined as

$$\begin{aligned}
&\lambda^i(z_i) = \lambda_0^i e^{k_i z_i}, \qquad G^i(z_i) = G_0^i e^{k_i z_i},\\
&\lambda_0^i = \frac{\mu_i E_0^i}{(1+\mu_i)(1-2\mu_i)}, \qquad G_0^i = \frac{E_0^i}{2(1+\mu_i)}.
\end{aligned} \tag{2}$$

The equilibrium equations are

$$\begin{aligned}
&\frac{\partial \sigma_x^i}{\partial x} + \frac{\partial \tau_{xy}^i}{\partial y} + \frac{\partial \tau_{xz_i}^i}{\partial z_i} = 0, \qquad \frac{\partial \sigma_y^i}{\partial y} + \frac{\partial \tau_{xy}^i}{\partial x} + \frac{\partial \tau_{yz_i}^i}{\partial z_i} = 0,\\
&\frac{\partial \sigma_{z_i}^i}{\partial z_i} + \frac{\partial \tau_{xz_i}^i}{\partial x} + \frac{\partial \tau y_{xz_i}^i}{\partial y} = 0.
\end{aligned} \tag{3}$$

Substituting Eq. (1) into Eq. (3), one has

$$\begin{aligned}
&(\lambda_0^i + 2G_0^i)\frac{\partial^2 w^i}{\partial z_i^2} + G_0^i \frac{\partial^2 w^i}{\partial x^2} + G_0^i \frac{\partial^2 w^i}{\partial y^2}\\
&+ (\lambda_0^i + G_0^i)\frac{\partial^2 u^i}{\partial x \partial z_i} + (\lambda_0^i + G_0^i)\frac{\partial^2 v^i}{\partial y \partial z_i}\\
&+ k_i \lambda_0^i \left(\frac{\partial u^i}{\partial x} + \frac{\partial v^i}{\partial y}\right) + k_i(\lambda_0^i + 2G_0^i)\frac{\partial w^i}{\partial z_i} = 0,\\
&(\lambda_0^i + 2G_0^i)\frac{\partial^2 u^i}{\partial x^2} + G_0^i \frac{\partial^2 u^i}{\partial y^2} + G_0^i \frac{\partial^2 u^i}{\partial z_i^2}\\
&+ (\lambda_0^i + G_0^i)\frac{\partial^2 v^i}{\partial x \partial y} + (\lambda_0^i + G_0^i)\frac{\partial^2 w^i}{\partial x \partial z_i}\\
&+ k_i G_0^i \left(\frac{\partial u^i}{\partial z_i} + \frac{\partial w^i}{\partial x}\right) = 0,\\
&(\lambda_0^i + 2G_0^i)\frac{\partial^2 v^i}{\partial y^2} + G_0^i \frac{\partial^2 v^i}{\partial x^2} + G_0^i \frac{\partial^2 v^i}{\partial z_i^2}\\
&+ (\lambda_0^i + G_0^i)\frac{\partial^2 u^i}{\partial x \partial y} + (\lambda_0^i + G_0^i)\frac{\partial^2 w^i}{\partial y \partial z_i}\\
&+ k_i G_0^i \left(\frac{\partial v^i}{\partial z_i} + \frac{\partial w^i}{\partial y}\right) = 0.
\end{aligned} \tag{4}$$

The simply supported boundary conditions can be expressed as (Wu *et al*. 2017)

$$\begin{aligned}
&\sigma_x^i = v^i = w^i = 0 \qquad \text{at} \qquad x = 0, a,\\
&\sigma_y^i = u^i = w^i = 0 \qquad \text{at} \qquad y = 0, b.
\end{aligned} \tag{5}$$

The displacement components are expanded into double Fourier series

$$\begin{aligned}
u^i(x, y, z_i) &= \sum_{m=1}^{\infty}\sum_{n=1}^{\infty} U_{mn}^i(z_i)\cos\left(\frac{m\pi x}{a}\right)\sin\left(\frac{n\pi y}{b}\right),\\
v^i(x, y, z_i) &= \sum_{m=1}^{\infty}\sum_{n=1}^{\infty} V_{mn}^i(z_i)\sin\left(\frac{m\pi x}{a}\right)\cos\left(\frac{n\pi y}{b}\right),\\
w^i(x, y, z_i) &= \sum_{m=1}^{\infty}\sum_{n=1}^{\infty} W_{mn}^i(z_i)\sin\left(\frac{m\pi x}{a}\right)\sin\left(\frac{n\pi y}{b}\right),
\end{aligned} \tag{6}$$

Substituting Eq. (6) into Eq. (4), one has

$$\begin{aligned}
&(\lambda_0^i + G_0^i)\left(\frac{m\pi}{a}\frac{dU_{mn}^i(z_i)}{dz_i} + \frac{n\pi}{b}\frac{dV_{mn}^i(z_i)}{dz_i}\right)\\
&+ k_i \lambda_0^i \left(\frac{m\pi}{a}U_{mn}^i(z_i) + \frac{n\pi}{b}V_{mn}^i(z_i)\right)\\
&= (\lambda_0^i + 2G_0^i)\frac{d^2 W_{mn}^i(z_i)}{dz_i^2} + k_i(\lambda_0^i + 2G_0^i)\frac{dW_{mn}^i(z_i)}{dz_i}\\
&- G_0^i\left[\left(\frac{m\pi}{a}\right)^2 + \left(\frac{n\pi}{b}\right)^2\right]W_{mn}^i(z_i),
\end{aligned} \tag{7}$$

$$\begin{aligned}
&\left[(\lambda_0^i+2G_0^i)\left(\frac{m\pi}{a}\right)^2+G_0^i\left(\frac{n\pi}{b}\right)^2\right]U_{mn}^i(z_i)\\
&-k_iG_0^i\frac{dU_{mn}^i(z_i)}{dz_i}-G_0^i\frac{d^2U_{mn}^i(z_i)}{dz_i^2}\\
&+(\lambda_0^i+G_0^i)\frac{mn\pi^2}{ab}V_{mn}^i(z_i)\\
&=(\lambda_0^i+G_0^i)\frac{m\pi}{a}\frac{dW_{mn}^i(z_i)}{dz_i}+k_iG_0^i\frac{m\pi}{a}W_{mn}^i(z_i),\\
&\left[(\lambda_0^i+2G_0^i)\left(\frac{n\pi}{b}\right)^2+G_0^i\left(\frac{m\pi}{a}\right)^2\right]V_{mn}^i(z_i)\\
&-k_iG_0^i\frac{dV_{mn}^i(z_i)}{dz_i}-G_0^i\frac{d^2V_{mn}^i(z_i)}{dz_i^2}\\
&+(\lambda_0^i+G_0^i)\frac{mn\pi^2}{ab}U_{mn}^i(z_i)\\
&=(\lambda_0^i+G_0^i)\frac{n\pi}{b}\frac{dW_{mn}^i(z_i)}{dz_i}+k_iG_0^i\frac{n\pi}{b}W_{mn}^i(z_i).
\end{aligned}\tag{7}$$

By eliminating $U_{mn}^i(z_i)$ and $V_{mn}^i(z_i)$ in Eq. (7), a fourth-order differential equation of $W_{mn}^i(z_i)$ is obtained as follows

$$\begin{aligned}
&\frac{d^4W_{mn}^i(z_i)}{dz_i^4}+2k_i\frac{d^3V_{mn}^i(z_i)}{dz_i^3}+(k_i^2-2\alpha_{mn}^2)\frac{d^2W_{mn}^i(z_i)}{dz_i^2}\\
&-2k_i\alpha_{mn}^2\frac{dW_{mn}^i(z_i)}{dz_i}+(\alpha_{mn}^4+\frac{k_i^2\alpha_{mn}^2\lambda_0^i}{\lambda_0^i+2G_0^i})W_{mn}^i(z_i)=0,
\end{aligned}\tag{8}$$

where $\alpha_{mn}=\sqrt{(m\pi/a)^2+(n\pi/b)^2}$. The solution of the above equation is

$$\begin{aligned}
W_{mn}^i(z_i)&=e^{r_{mn}z_i}\cos(t_{mn}z_i)A_{mn}^i+e^{r_{mn}z_i}\sin(t_{mn}z_i)B_{mn}^i\\
&+e^{s_{mn}z_i}\cos(t_{mn}z_i)C_{mn}^i+e^{s_{mn}z_i}\sin(t_{mn}z_i)D_{mn}^i,
\end{aligned}\tag{9}$$

where A_{mn}^i, B_{mn}^i, C_{mn}^i and D_{mn}^i are the undecided coefficients and

$$\begin{aligned}
r_{mn}&=-0.5k_i+\{0.5\alpha_{mn}^2+0.125k_i^2+[(0.5\alpha_{mn}^2+0.125k_i^2)^2\\
&\quad+0.25\lambda_0^ik_i^2\alpha_{mn}^2/(\lambda_0^i+G_0^i)]^{0.5}\}^{0.5},\\
s_{mn}&=-0.5k_i-\{0.5\alpha_{mn}^2+0.125k_i^2+[(0.5\alpha_{mn}^2+0.125k_i^2)^2\\
&\quad+0.25\lambda_0^ik_i^2\alpha_{mn}^2/(\lambda_0^i+2G_0^i)]^{0.5}\}^{0.5},\\
t_{mn}&=\{-(0.5\alpha_{mn}^2+0.125k_i^2)+[(0.5\alpha_{mn}^2+0.125k_i^2)^2\\
&\quad+0.25\lambda_0^ik_i^2\alpha_{mn}^2/(\lambda_0^i+2G_0^i)]^{0.5}\}^{0.5}.
\end{aligned}$$

Identically, $U_{mn}^i(z_i)$ and $V_{mn}^i(z_i)$ can also be derived out, as follows

$$\begin{aligned}
U_{mn}^i(z_i)&=[(T_{mn}^1R_{mn}^1+T_{mn}^2R_{mn}^2)\cos(t_{mn}z_i)\\
&\quad+(T_{mn}^2R_{mn}^1-T_{mn}^1R_{mn}^2)\sin(t_{mn}z_i)]e^{r_{mn}z_i}A_{mn}^i\\
&\quad+[(T_{mn}^1R_{mn}^2-T_{mn}^2R_{mn}^1)\cos(t_{mn}z_i)\\
&\quad+(T_{mn}^2R_{mn}^2+T_{mn}^1R_{mn}^1)\sin(t_{mn}z_i)]e^{r_{mn}z_i}B_{mn}^i\\
&\quad+[(T_{mn}^3R_{mn}^3+T_{mn}^4R_{mn}^4)\cos(t_{mn}z_i)\\
&\quad+(T_{mn}^4R_{mn}^3-T_{mn}^3R_{mn}^4)\sin(t_{mn}z_i)]e^{s_{mn}z_i}C_{mn}^i\\
&\quad+[(T_{mn}^3R_{mn}^4-T_{mn}^4R_{mn}^3)\cos(t_{mn}z_i)\\
&\quad+(T_{mn}^4R_{mn}^4+T_{mn}^3R_{mn}^3)\sin(t_{mn}z_i)]e^{s_{mn}z_i}D_{mn}^i\\
&\quad+e^{p_{mn}z_i}E_{mn}^i+e^{q_{mn}z_i}F_{mn}^i.
\end{aligned}\tag{10}$$

where E_{mn}^i and F_{mn}^i are the undecided coefficients and the details of T_{mn}^*, R_{mn}^*, p_{mn} and q_{mn} are given in Eq. (A1) in Appendix. Substituting Eqs. (8), (10) and (11) into Eq. (1), the expressions of stresses are derived out

$$\begin{aligned}
&V_{mn}^i(z_i)=\\
&\{[(R_{mn}^5-\frac{m\pi}{a}(T_{mn}^1R_{mn}^1+T_{mn}^2R_{mn}^2)\cos(t_{mn}z_i)\\
&-[R_{mn}^6+\frac{m\pi}{a}(T_{mn}^2R_{mn}^1-T_{mn}^1R_{mn}^2)]\\
&\quad\sin(t_{mn}z_i)\}\frac{b}{n\pi}e^{r_{mn}z_i}A_{mn}^i\\
&+\{[R_{mn}^6-\frac{m\pi}{a}(T_{mn}^1R_{mn}^2-T_{mn}^2R_{mn}^1)]\cos(t_{mn}z_i)\\
&+[R_{mn}^5-\frac{m\pi}{a}(T_{mn}^2R_{mn}^2+T_{mn}^1R_{mn}^1)]\\
&\quad\sin(t_{mn}z_i)\}\frac{b}{n\pi}e^{r_{mn}z_i}B_{mn}^i\\
&+\{[R_{mn}^7-\frac{m\pi}{a}(T_{mn}^3R_{mn}^3+T_{mn}^4R_{mn}^4)]\cos(t_{mn}z_i)\\
&-[R_{mn}^8+\frac{m\pi}{a}(T_{mn}^4R_{mn}^3-T_{mn}^3R_{mn}^4)]\\
&\quad\sin(t_{mn}z_i)\}\frac{b}{n\pi}e^{s_{mn}z_i}C_{mn}^i\\
&+\{[R_{mn}^8-\frac{m\pi}{a}(T_{mn}^3R_{mn}^4-T_{mn}^4R_{mn}^3)]\cos(t_{mn}z_i)\\
&+[R_{mn}^7-\frac{m\pi}{a}(T_{mn}^4R_{mn}^4+T_{mn}^3R_{mn}^3)]\\
&\quad\sin(t_{mn}z_i)\}\frac{b}{n\pi}e^{s_{mn}z_i}D_{mn}^i\\
&-\frac{bm}{an}e^{p_{mn}z_i}E_{mn}^i-\frac{bm}{an}e^{q_{mn}z_i}F_{mn}^i,
\end{aligned}\tag{11}$$

$$\begin{aligned}
&\sigma_x^i(x,y,z_i)=\\
&-\sum_{m=1}^{\infty}\sum_{n=1}^{\infty}\sin\frac{m\pi x}{a}\sin\frac{n\pi y}{b}\\
&\times\{[I_{mn}^1\cos(t_{mn}z_i)+I_{mn}^2\cos(t_{mn}z_i)]e^{(r_{mn}+k_i)z_i}A_{mn}^i\\
&+[I_{mn}^1\sin(t_{mn}z_i)-I_{mn}^2\cos(t_{mn}z_i)]e^{(r_{mn}+k_i)z_i}B_{mn}^i\\
&+[I_{mn}^3\cos(t_{mn}z_i)+I_{mn}^4\sin(t_{mn}z_i)]e^{(s_{mn}+k_i)z_i}C_{mn}^i\\
&+[I_{mn}^3\sin(t_{mn}z_i)-I_{mn}^4\cos(t_{mn}z_i)]e^{(s_{mn}+k_i)z_i}D_{mn}^i\\
&+\frac{2m\pi}{a}G_0^ie^{(p_{mn}+k_i)z_i}E_{mn}^i+\frac{2m\pi}{a}G_0^ie^{(q_{mn}+k_i)z_i}F_{mn}^i\},
\end{aligned}\tag{12}$$

$$\begin{aligned}\sigma_y^i(x,y,z_i) &= -\sum_{m=1}^{\infty}\sum_{n=1}^{\infty}\sin\frac{m\pi x}{a}\sin\frac{n\pi y}{b}\\ &\times\{[J_{mn}^1\cos(t_{mn}z_i)+J_{mn}^2\cos(t_{mn}z_i)]e^{(r_{mn}+k_i)z_i}A_{mn}^i\\ &+[J_{mn}^1\sin(t_{mn}z_i)-J_{mn}^2\cos(t_{mn}z_i)]e^{(r_{mn}+k_i)z_i}B_{mn}^i\\ &+[J_{mn}^3\cos(t_{mn}z_i)+J_{mn}^4\sin(t_{mn}z_i)]e^{(s_{mn}+k_i)z_i}C_{mn}^i\\ &+[J_{mn}^3\sin(t_{mn}z_i)-J_{mn}^4\cos(t_{mn}z_i)]e^{(s_{mn}+k_i)z_i}D_{mn}^i\\ &+\frac{2m\pi}{a}G_0^ie^{(p_{mn}+k_i)z_i}E_{mn}^i-\frac{2m\pi}{a}G_0^ie^{(q_{mn}+k_i)z_i}F_{mn}^i\},\end{aligned}$$

$$\begin{aligned}\sigma_{z_i}^i(x,y,z_i) &= \sum_{m=1}^{\infty}\sum_{n=1}^{\infty}\sin\frac{m\pi x}{a}\sin\frac{n\pi y}{b}\\ &\times\{[K_{mn}^1\cos(t_{mn}z_i)+K_{mn}^2\sin(t_{mn}z_i)]e^{(r_{mn}+k_i)z_i}A_{mn}^i\\ &+[K_{mn}^1\sin(t_{mn}z_i)-K_{mn}^2\cos(t_{mn}z_i)]e^{(r_{mn}+k_i)z_i}B_{mn}^i\\ &+[K_{mn}^3\cos(t_{mn}z_i)+K_{mn}^4\sin(t_{mn}z_i)]e^{(s_{mn}+k_i)z_i}C_{mn}^i\\ &+[K_{mn}^3\sin(t_{mn}z_i)-K_{mn}^4\cos(t_{mn}z_i)]e^{(s_{mn}+k_i)z_i}D_{mn}^i\},\end{aligned}$$

$$\begin{aligned}\tau_{xy}^i(x,y,z_i) &= \sum_{m=1}^{\infty}\sum_{n=1}^{\infty}\cos\frac{m\pi x}{a}\cos\frac{n\pi y}{b}\\ &\times\{[L_{mn}^1\cos(t_{mn}z_i)+L_{mn}^2\sin(t_{mn}z_i)]e^{(r_{mn}+k_i)z_i}A_{mn}^i\\ &+[L_{mn}^1\sin(t_{mn}z_i)-L_{mn}^2\cos(t_{mn}z_i)]e^{(r_{mn}+k_i)z_i}B_{mn}^i\\ &+[L_{mn}^3\cos(t_{mn}z_i)+L_{mn}^4\sin(t_{mn}z_i)]e^{(s_{mn}+k_i)z_i}C_{mn}^i\\ &+[L_{mn}^3\sin(t_{mn}z_i)-L_{mn}^4\cos(t_{mn}z_i)]e^{(s_{mn}+k_i)z_i}D_{mn}^i\\ &+\frac{bG_0^i}{n\pi}\left(\frac{n^2\pi^2}{b^2}-\frac{m^2\pi^2}{a^2}\right)e^{(p_{mn}+k_i)z_i}E_{mn}^i\\ &+\frac{bG_0^i}{n\pi}\left(\frac{n^2\pi^2}{b^2}-\frac{m^2\pi^2}{a^2}\right)e^{(q_{mn}+k_i)z_i}F_{mn}^i\},\end{aligned}\tag{12}$$

$$\begin{aligned}\tau_{xz_i}^i(x,y,z_i) &= \sum_{m=1}^{\infty}\sum_{n=1}^{\infty}\cos\frac{m\pi x}{a}\sin\frac{n\pi y}{b}\\ &\times\{[M_{mn}^1\cos(t_{mn}z_i)+M_{mn}^2\sin(t_{mn}z_i)]e^{(r_{mn}+k_i)z_i}A_{mn}^i\\ &+[M_{mn}^1\sin(t_{mn}z_i)-M_{mn}^2\cos(t_{mn}z_i)]e^{(r_{mn}+k_i)z_i}B_{mn}^i\\ &+[M_{mn}^3\cos(t_{mn}z_i)+M_{mn}^4\sin(t_{mn}z_i)]e^{(s_{mn}+k_i)z_i}C_{mn}^i\\ &+[M_{mn}^3\sin(t_{mn}z_i)-M_{mn}^4\cos(t_{mn}z_i)]e^{(s_{mn}+k_i)z_i}D_{mn}^i\\ &+G_0^ip_{mn}e^{(p_{mn}+k_i)z_i}E_{mn}^i+G_0^iq_{mn}e^{(q_{mn}+k_i)z_i}F_{mn}^i\},\end{aligned}$$

$$\begin{aligned}\tau_{yz_i}^i(x,y,z_i) &= \sum_{m=1}^{\infty}\sum_{n=1}^{\infty}\sin\frac{m\pi x}{a}\cos\frac{n\pi y}{b}\\ &\times\{[N_{mn}^1\cos(t_{mn}z_i)+N_{mn}^2\sin(t_{mn}z_i)]e^{(r_{mn}+k_i)z_i}A_{mn}^i\\ &+[N_{mn}^1\sin(t_{mn}z_i)-N_{mn}^2\cos(t_{mn}z_i)]e^{(r_{mn}+k_i)z_i}B_{mn}^i\\ &+[N_{mn}^3\cos(t_{mn}z_i)+N_{mn}^4\sin(t_{mn}z_i)]e^{(s_{mn}+k_i)z_i}C_{mn}^i\\ &+[N_{mn}^3\sin(t_{mn}z_i)-N_{mn}^4\cos(t_{mn}z_i)]e^{(s_{mn}+k_i)z_i}D_{mn}^i\\ &+\frac{mbG_0^i}{na}p_{mn}e^{(p_{mn}+k_i)z_i}E_{mn}^i-\frac{mbG_0^i}{na}q_{mn}e^{(q_{mn}+k_i)z_i}F_{mn}^i\},\end{aligned}$$

in which, the details of I_{mn}^*, J_{mn}^*, K_{mn}^*, L_{mn}^*, M_{mn}^* and N_{mn}^* are given in Eq. (A2) in Appendix.

2.2 Load conditions and continuous conditions

The load acting on the plate surfaces can be described as

$$\begin{aligned}&\sigma_{z_p}^p(x,y,h_p)=-q(x,y), && \tau_{xz_p}^p(x,y,h_p)=0,\\ &\tau_{yz_p}^p(x,y,h_p)=0, && \sigma_{z_1}^1(x,y,0)=0,\\ &\tau_{xz_1}^1(x,y,0)=0, && \tau_{yz_1}^1(x,y,0)=0,\end{aligned}\tag{13}$$

in which, the load function $q(x, y)$ is expanded into double Fourier series form, as follows

$$\begin{aligned}q(x,y) &= \sum_{m=1}^{\infty}\sum_{n=1}^{\infty}Q_{mn}\sin(\frac{m\pi x}{a})\sin(\frac{n\pi y}{b}),\\ Q_{mn} &= \frac{4}{ab}\int_0^a\int_0^b q(x,y)\sin(\frac{m\pi x}{a})\sin(\frac{n\pi y}{b})dxdy.\end{aligned}\tag{14}$$

The adjacent layers are perfectly connected at the interface, i.e.

$$\begin{aligned}\sigma_{z_i}^i(x,y,h_i) &= \sigma_{z_{i+1}}^{i+1}(x,y,0),\\ \tau_{xz_i}^i(x,y,h_i) &= \tau_{xz_{i+1}}^{i+1}(x,y,0),\\ \tau_{yz_i}^i(x,y,h_i) &= \tau_{yz_{i+1}}^{i+1}(x,y,0),\\ u^i(x,y,h_i) &= u^{i+1}(x,y,0),\\ v^i(x,y,h_i) &= v^{i+1}(x,y,0),\\ w^i(x,y,h_i) &= w^{i+1}(x,y,0).\end{aligned}\tag{15}$$

2.3 Recursive matrix

The stress and displacement components in Eqs. (11) and (12) are rearranged into the vector form, as follows

$$\begin{aligned}&\begin{bmatrix}u^i(x,y,z_i)\\ v^i(x,y,z_i)\\ w^i(x,y,z_i)\\ \sigma_{z_i}^i(x,y,z_i)\\ \tau_{xz_i}^i(x,y,z_i)\\ \tau_{yz_i}^i(x,y,z_i)\end{bmatrix}\\ &=\sum_{m=1}^{\infty}\sum_{n=1}^{\infty}\begin{bmatrix}U_{mn}^i(z_i)\cos(m\pi x/a)\sin(n\pi y/b)\\ V_{mn}^i(z_i)\sin(m\pi x/a)\cos(n\pi y/b)\\ W_{mn}^i(z_i)\sin(m\pi x/a)\sin(n\pi y/b)\\ Z_{mn}^i(z_i)\sin(m\pi x/a)\sin(n\pi y/b)\\ X_{mn}^i(z_i)\cos(m\pi x/a)\sin(n\pi y/b)\\ Y_{mn}^i(z_i)\sin(m\pi x/a)\cos(n\pi y/b)\end{bmatrix},\end{aligned}\tag{16}$$

where $U^i_{mn}(z_i)$, $V^i_{mn}(z_i)$, $W^i_{mn}(z_i)$, $Z^i_{mn}(z_i)$, $X^i_{mn}(z_i)$ and $Y^i_{mn}(z_i)$ can be derived out by substituting Eqs. (11) and (12) into Eq. (16), as follows

$$\Psi^i_{mn}(z_i) = \Gamma^i_{mn}(z_i)\Omega^i_{mn}, \tag{17}$$

in which

$$\Psi^i_{mn}(z_i) = \left[U^i_{mn}(z_i)\ V^i_{mn}(z_i)\ W^i_{mn}(z_i)\ Z^i_{mn}(z_i)\ X^i_{mn}(z_i)\ Y^i_{mn}(z_i)\right]^T,$$

$$\Omega^i_{mn} = \left[A^i_{mn}\ B^i_{mn}\ C^i_{mn}\ D^i_{mn}\ E^i_{mn}\ F^i_{mn}\right]^T,$$

$$\Omega^i_{mn} = \left[A^i_{mn}\ B^i_{mn}\ C^i_{mn}\ D^i_{mn}\ E^i_{mn}\ F^i_{mn}\right]^T,$$

$$\Gamma^i_{mn}(z_i) = \begin{bmatrix} f^{11}_{mn}(z_i) & f^{12}_{mn}(z_i) & f^{13}_{mn}(z_i) & f^{14}_{mn}(z_i) & f^{15}_{mn}(z_i) & f^{16}_{mn}(z_i) \\ f^{21}_{mn}(z_i) & f^{22}_{mn}(z_i) & f^{23}_{mn}(z_i) & f^{24}_{mn}(z_i) & f^{25}_{mn}(z_i) & f^{26}_{mn}(z_i) \\ f^{31}_{mn}(z_i) & f^{32}_{mn}(z_i) & f^{33}_{mn}(z_i) & f^{34}_{mn}(z_i) & 0 & 0 \\ f^{41}_{mn}(z_i) & f^{42}_{mn}(z_i) & f^{43}_{mn}(z_i) & f^{44}_{mn}(z_i) & 0 & 0 \\ f^{51}_{mn}(z_i) & f^{52}_{mn}(z_i) & f^{53}_{mn}(z_i) & f^{54}_{mn}(z_i) & f^{55}_{mn}(z_i) & f^{56}_{mn}(z_i) \\ f^{61}_{mn}(z_i) & f^{62}_{mn}(z_i) & f^{63}_{mn}(z_i) & f^{64}_{mn}(z_i) & f^{65}_{mn}(z_i) & f^{66}_{mn}(z_i) \end{bmatrix},$$

where the elements in the matrix $\Gamma^i_{mn}(z_i)$ are defined in Eq. (A3) in Appendix. By taking z_i as 0 and h_i in Eq. (17), respectively, we have

$$\begin{aligned} \Psi^i_{mn}(0) &= \Gamma^i_{mn}(0)\Omega^i_{mn}, \\ \Psi^i_{mn}(h_i) &= \Gamma^i_{mn}(h_i)\Omega^i_{mn}. \end{aligned} \tag{18}$$

Elimination of Ω^i_{mn} in Eq. (18) gives

$$\Psi^i_{mn}(h_i) = \Gamma^i_{mn}(h_i)\Gamma^i_{mn}{}^{-1}(0)\Psi^i_{mn}(0). \tag{19}$$

The continuous conditions of Eq. (15) are rewritten as

$$\Psi^{i+1}_{mn}(0) = \Psi^i_{mn}(h_i). \tag{20}$$

Combination of Eq. (19) with Eq. (20) yields a relationship of stresses and displacements between the top surface and the bottom surface of the plate

$$\Psi^p_{mn}(h_p) = \left[\prod_{i=p}^{1}\Gamma^i_{mn}(h_i)\Gamma^i_{mn}{}^{-1}(0)\right]\Psi^i_{mn}(0). \tag{21}$$

We define

$$\begin{bmatrix} S^{11}_{mn} & S^{12}_{mn} \\ S^{21}_{mn} & S^{22}_{mn} \end{bmatrix} = \prod_{i=p}^{1}\Gamma^i_{mn}(h_i)\Gamma^i_{mn}{}^{-1}(0), \tag{22}$$

where S^{11}_{mn}, S^{12}_{mn}, S^{21}_{mn} and S^{22}_{mn} are the 3×3 sub-matrixes. Thus, Eq. (21) becomes

$$\begin{bmatrix} U^p_{mn}(h_p) \\ V^p_{mn}(h_p) \\ W^p_{mn}(h_p) \\ Z^p_{mn}(h_p) \\ X^p_{mn}(h_p) \\ Y^p_{mn}(h_p) \end{bmatrix} = \begin{bmatrix} S^{11}_{mn} & S^{12}_{mn} \\ S^{21}_{mn} & S^{22}_{mn} \end{bmatrix} \begin{bmatrix} U^1_{mn}(0) \\ V^1_{mn}(0) \\ W^1_{mn}(0) \\ Z^1_{mn}(0) \\ X^1_{mn}(0) \\ Y^1_{mn}(0) \end{bmatrix}. \tag{23}$$

According to the loading conditions of Eq. (13), one has

$$\begin{aligned} &X^p_{mn}(h_p) = 0, \quad Y^p_{mn}(h_p) = 0, \quad Z^p_{mn}(h_p) = -Q_{nm}, \\ &X^1_{mn}(0) = 0, \quad Y^1_{mn}(0) = 0, \quad Z^1_{mn}(0) = 0. \end{aligned} \tag{24}$$

Decomposing Eq. (23), two equations are obtained

$$\begin{aligned} S^{11}_{mn}\begin{bmatrix} U^1_{mn}(0) \\ V^1_{mn}(0) \\ W^1_{mn}(0) \end{bmatrix} &= \begin{bmatrix} U^p_{mn}(h_p) \\ V^p_{mn}(h_p) \\ W^p_{mn}(h_p) \end{bmatrix}, \\ S^{21}_{mn}\begin{bmatrix} U^1_{mn}(0) \\ V^1_{mn}(0) \\ W^1_{mn}(0) \end{bmatrix} &= \begin{bmatrix} -Q_{mn} \\ 0 \\ 0 \end{bmatrix}. \end{aligned} \tag{25}$$

The solution of the second equation in Eq. (25) is

$$\begin{bmatrix} U^1_{mn}(0) \\ V^1_{mn}(0) \\ W^1_{mn}(0) \end{bmatrix} = (S^{21}_{mn})^{-1}\begin{bmatrix} -Q_{mn} \\ 0 \\ 0 \end{bmatrix}. \tag{26}$$

Combining Eq. (19) with Eq. (20), $\Psi^p_{mn}(h_p)$ can be derived out, as follows

$$\Psi^i_{mn}(h_i) = \left[\prod_{j=i}^{1}\Gamma^j_{mn}(h_j)\Gamma^j_{mn}{}^{-1}(0)\right]\Psi^1_{mn}(0). \tag{27}$$

Finally, the coefficients in the stress and displacement components can be determined

$$\Omega^i_{mn} = \Gamma^i_{mn}{}^{-1}(h_i)\Psi^i_{mn}(h_i). \tag{28}$$

By substituting the coefficients back into Eqs. (11) and (12), the solution of stresses and displacements of the plate is obtained finally.

It should be mentioned that as the layer number p increases, only the computation effort in Eq. (22) increases slightly. Thus, the present method is computational efficiently for plates with any number of layers. Moreover, the present method can be extended to plates with other boundary conditions. For example, the clamped end can be equivalent to the simply supported one acted by the unknown horizontal reaction which can be determined from the zero displacement condition at the clamped end (Xu *et al*. 2008).

3. Numerical examples

In the following examples, the series terms in stress and displacement components are truncated up to N, i.e., m, n = 1, 2, 3... N. The elastic modulus in the permeation layer is determined by the adjacent layers, as follows

$$E_i(z_i) = E_{i-1} e^{\frac{z_i}{h_i}\ln(E_{i+1}/E_{i-1})}. \tag{29}$$

The location of the plate is identified by the global coordinate system O-xyz

$$z = z_i + \sum_{j=1}^{i-1} h_j. \tag{30}$$

3.1 Convergence and comparison studies

Consider a refined sandwich plate composed of nine layers with dimensions a = 1500 mm, b = 700 mm and H = 200 mm, subjected to uniform load with $q(x, y)$ = 1 N/mm^2 acting on the top surface. The layer distribution along the thickness direction is shown in Fig. 2. The thickness, elastic modulus and Poisson's ratio of each layer are listed in Table 1. The solutions of stresses and displacements with different series terms N = 1, 2…15, are given in Table 2. It can be seen from Table 2 that the present solution is rapidly convergent and are highly accurate with at least three significant digits when N = 15. Thus, the term of number is fixed at N=15 for the following calculations.

It is well known that the reliability and accuracy of numerical solutions such as the FE solutions should be checked and evaluated through the comparison study with the strict solutions. The present solution is compared with the FE solution obtained from the software ANSYS. Consider the plate described in Section 3.1, however, subjected to sinusoidal load with $q(x, y) = \sin(\pi x / a)\sin(\pi y / b)$ N/mm^2. In the FE model, each permeation layer is equivalent to n homogeneous layers along the thickness. The SOLID-185 element is employed to model all the plate layers. The FE mesh of each layer is created by dividing its length into 150 elements, its width into 70 elements, while the thicknesses of layers 1, 2, 3…9 are, respectively, divided into 4, n, 1, n, 12, n, 1, n, 4 elements. The FE results for different n are compared with present ones, as shown in Table 3. It can be found from Table 3 that the FE results tend to be convergent and close to the present ones with the increase of n. The errors of σ_0, τ_0 and w_0 are 1.84%, 0.948% and 1.34% when n = 25. However, the FE method becomes computationally expensive when n is large.

By letting k_i = 0 in the expression of $E_i(z_i)$, the FGM layer in the plate degenerates to the isotropic one. Consider a sandwich plate, which was studied by Foraboschi (2013) using the two-dimensional Kirchhoff-Love (KL) plate

Table 1 The thickness, elastic modulus and Poisson's ratio for a nine-layer refine sandwich plate

i	h_i [mm]	E_i (Mpa)	μ_i
1	18	20950	0.25
2	10	$E_1 e^{[z_2 \ln(E_3/E_1)]/h_2}$	0.25
3	2	3500	0.25
4	10	$E_3 e^{[z_4 \ln(E_5/E_3)]/h_4}$	0.25
5	120	70	0.25
6	10	$E_5 e^{[z_6 \ln(E_7/E_5)]/h_6}$	0.25
7	2	3500	0.25
8	10	$E_7 e^{[z_8 \ln(E_9/E_7)]/h_8}$	0.25
9	18	20950	0.25

Table 2 Convergence study of the present results σ_x^1, w^1 at x = 750 mm, y = 350 mm, z = 0 and σ_z^1, τ_{xz}^1, τ_{xy}^1 at x = 375 mm, y = 175 mm, z = 18 mm

N	σ_x^1	σ_z^1	τ_{xz}^1	τ_{xy}^1	w^1
1	24.62	-0.0781	-0.5079	1.450	-7.556
3	14.77	-0.1377	-0.2612	0.7811	-6.835
5	17.39	-0.1175	-0.1614	0.6530	-6.913
7	16.84	-0.1104	-0.1902	0.6714	-6.904
9	16.95	-0.1126	-0.1975	0.6737	-6.905
11	16.93	-0.1133	-0.1956	0.6734	-6.905
13	16.93	-0.1131	-0.1951	0.6734	-6.905
15	16.93	-0.1130	-0.1952	0.6734	-6.905

*Note: The units of stresses and displacements are [Mpa] and [mm], respectively

Table 3 Comparison of stresses and displacements between the present solution and the FE one

	FE solution with different n						Present solution
n	2	4	6	10	15	25	
σ_0 [Mpa]	-1.542	-1.938	-2.137	-2.245	-2.293	-2.295	-2.338
Error (%)	34.0	17.1	8.6	3.97	1.92	1.84	/
τ_0 [Mpa]	-0.6250	-0.6262	-0.6265	-0.6266	-0.6266	-0.6266	-0.6326
Error (%)	1.20	1.01	0.972	0.952	0.946	0.948	/
w_0 [mm]	-4.642	-4.660	-4.664	-4.666	-4.666	-4.667	-4.730
Error (%)	1.86	1.48	1.40	1.36	1.35	1.34	/

*Note: σ_0 is σ_x^2 at x = 750 mm, y = 350 mm, z = 18 mm, τ_0 is τ_{xz}^2 at x = 0, y = 350 mm, z = 18 mm and w_0 is w^2 at x = 750 mm, y = 350 mm, z = 18 mm. The error = |(FE-Present)/Present

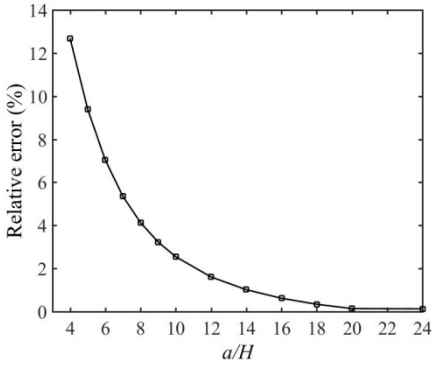

Fig. 4 Comparisons of w_m between the present solution and KL solution for different length-to-thickness ratios a/H (*Note: Relative error denotes (KL-Present)/Present)

Table 4 The thickness, elastic modulus and Poisson's ratio for a seven-layer refine sandwich plate

i	h_i [mm]	E_i (Mpa)	μ_i
1	16	20950	0.25
2	4	3500	0.25
3	h_3	$E_2 e^{[z_3 \ln(E_4/E_2)]/h_3}$	0.25
4	60-2h_3	70	0.25
5	h_3	$E_4 e^{[z_5 \ln(E_6/E_4)]/h_5}$	0.25
6	4	3500	0.25
7	16	20950	0.25

theory. The parameters are taken as $q(x, y) = 1$ N/mm^2, $E_1 = E_3 = 58000$ Mpa, $E_2 = 500$ Mpa, $\mu_1 = \mu_3 = 0.3$, $\mu_2 = 0.2$, $a = b$, $h_1 = h_3 = 50$ mm, $h_2 = 0.5$ mm. The comparison of the maximum plate deflection w_m between the present solution and KL solution (Foraboschi 2013) for different length-to-thickness ratios a/H is given in Fig. 4. It can be observed from Fig. 4 that the KL solution is close to the present ones for thin plates. However, the error from KL solution increases with the increase of a/H, which reaches about 13% when $a/H = 4$.

3.2 Parametric study

Consider a refined sandwich square plate with dimensions $a = b = 1000$ mm and $H = 100$ mm, subjected to sinusoidal load with $q(x, y) = \sin(\pi x / a)\sin(\pi y / b)$ N/mm^2 acting on the top surface. Here, we only consider the permeation effect of the adhesive into the core layer, i.e., the permeation layers $i = 2, 8$ in Fig. 2 are neglected. The thickness, elastic modulus and Poisson's ratio of each layer are listed in Table 4. The stress and displacement distributions along the plate thickness for different permeation thicknesses $h_3 = 0, 5, 10, 15$ mm are plotted in Fig. 5. The special case $h_3 = 0$ means the traditional sandwich plate model which neglects the permeation effect of the adhesives. It can be found from Fig. 5 that (i) the distributions of σ_x^i and τ_{xz}^i in the permeation layer (80 mm $- h_3 \le z \le 80$ mm) become smooth with the increase of h_3; (ii) σ_z^i is less influenced by h_3; (iii) the deflection w^i decreases with the increase of h_3.

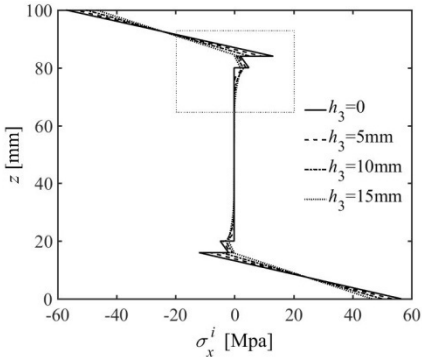

(a1) σ_x^i at $x = y = 500$ mm

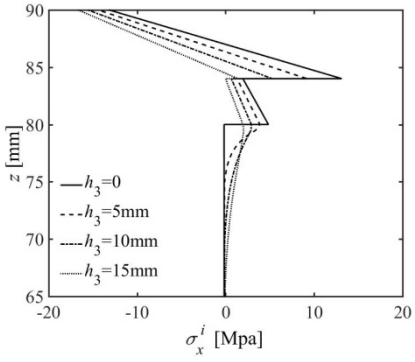

(a2) Enlarged view of σ_x^i

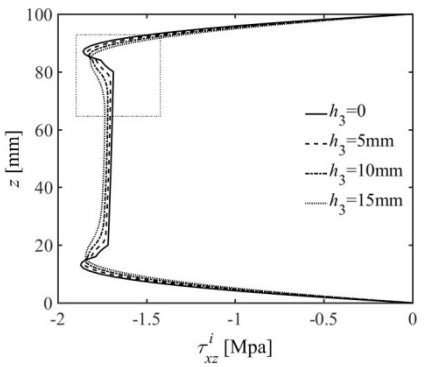

(b1) τ_{xz}^i at $x = 0, y = 500$ mm

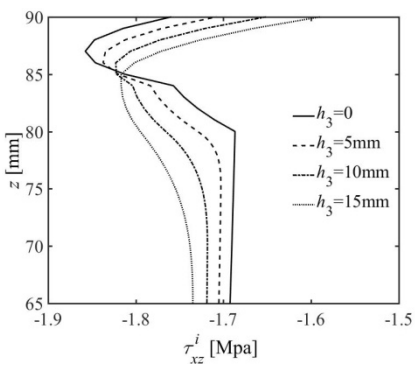

(b2) Enlarged view of τ_{xz}^i

Fig. 5 Distributions of stresses and displacement along the plate thickness for different permeation thicknesses $h_3 = 0, 5, 10, 15$ mm

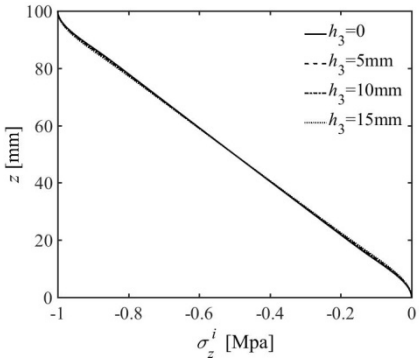

(*c*) σ_z^i at $x = y = 500$ mm

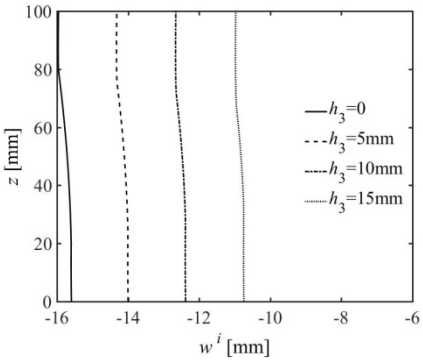

(*d*) w^i at $x = y = 500$ mm

Fig. 5 Continued

4. Conclusions

Based on the 3-D elasticity theory, a refined sandwich plate model which considers the permeation effect of adhesive is proposed. The solution of stress and displacement fields in the plate is obtained analytically. The boundary, loading conditions and continuous conditions are strictly satisfied. The following conclusions are summarized:

- By use of the recursive matrix method, the solution of stress and displacement for sandwich plate with many layers can be efficiently obtained.
- The present solution is rapidly convergent with high accuracy and is in good agreement with the finite element solution.
- The FE solution is close to the present one when the FGM layer in the FE model is divided into a series of homogeneous layers. However, the present method is more efficient than the FE method, in which the mesh division and computation are time-consuming.
- The solution based on the Kirchhoff-Love plate theory is in agreement with the present solution for thin plates, but has considerable error for thick plate.
- The permeation effect of adhesives has great effect on the stress and displacement distributions. The distributions of the longitudinal normal stress and the shear stress in the permeation layer become smooth in the thickness direction with the increase of the permeation thickness. The deflection decreases with the increase of the permeation thickness.

Acknowledgments

This work is financially supported by National Natural Science Foundation of China (Grant No. 51608264) and Key Program of National Natural Science Foundation of China (Grant No. 51238003).

References

Arani, A.G., Arani, H.K. and Maraghi, Z.K. (2016), "Vibration analysis of sandwich composite micro-plate under electro-magneto-mechanical loadings", *Appl. Math. Model.*, **40**(23), 10596-10615.

Belkorissat, I., Houari, M.S.A., Tounsi, A., Bedia, E.A. and Mahmoud, S.R. (2015), "On vibration properties of functionally graded nano-plate using a new nonlocal refined four variable model", *Steel. Compos. Struct., Int. J.*, **18**(4), 1063-1081.

Bouchafa, A., Bouiadjra, M.B., Houari, M.S.A. and Tounsi, A. (2015), "Thermal stresses and deflections of functionally graded sandwich plates using a new refined hyperbolic shear deformation theory", *Steel. Compos. Struct., Int. J.*, **18**(6), 1493-1515.

Bui, T.Q., Nguyen, M.N. and Zhang, C. (2011), "An efficient meshfree method for vibration analysis of laminated composite plates", *Comput. Mech.*, **48**(2), 175-193.

Bui, T.Q., Khosravifard, A., Zhang, C., Hematiyan, M.R. and Golub, M.V. (2013), "Dynamic analysis of sandwich beams with functionally graded core using a truly meshfree radial point interpolation method", *Eng. Struct.*, **47**, 90-104.

Bui, T.Q., Van Do, T., Ton, L.H.T., Doan, D.H., Tanaka, S., Pham, D.T., Nguyen-Van, T.A., Yu, Y. and Hirose, S. (2016), "On the high temperature mechanical behaviors analysis of heated functionally graded plates using FEM and a new third-order shear deformation plate theory", *Compos. Part B-Eng.*, **92**, 218-241.

Chen, W.Q. and Lee, K.Y. (2004), "Three-dimensional exact analysis of angle-ply laminates in cylindrical bending with interfacial damage via state-space method", *Compos. Struct.*, **64**(3), 275-283.

Civalek, Ö. (2017), "Free vibration of carbon nanotubes reinforced (CNTR) and functionally graded shells and plates based on FSDT via discrete singular convolution method", *Compos. Part B-Eng.*, **111**, 45-59.

Foraboschi, P. (2013), "Three-layered sandwich plate: Exact mathematical model", *Compos. Part B-Eng.*, **45**(1), 1601-1612.

Huang, Z. and Liew, J.Y. (2016), "Numerical studies of steel-concrete-steel sandwich walls with J-hook connectors subjected to axial loads", *Steel. Compos. Struct., Int. J.*, **21**(3), 461-477.

Iivani, M., MalekzadehFard, K. and Shokrollahi, S, (2016), "Higher order flutter analysis of doubly curved sandwich panels with variable thickness under aerothermoelastic loading", *Struct. Eng. Mech., Int. J.*, **60**(1), 1-19.

Isavand, S., Bodaghi, M., Shakeri, M. and Mohandesi, J.A. (2015), "Dynamic response of functionally gradient austenitic-ferritic steel composite panels under thermo-mechanical loadings", *Steel. Compos. Struct., Int. J.*, **18**(1), 1-28.

Li, J., Zheng, B., Yang, Q. and Hu, X. (2014), "Analysis on time-dependent behavior of laminated functionally graded beams with viscoelastic interlayer", *Compos. Struct.*, **107**, 30-35.

Li, D., Deng, Z. and Xiao, H. (2016), "Thermomechanical bending analysis of functionally graded sandwich plates using four-

variable refined plate theory", *Compos. Part B-Eng.*, **106**, 107-119.
Liu, S., Yu, T., Bui, T.Q., Yin, S., Thai, D.K. and Tanaka, S. (2017), "Analysis of functionally graded plates by a simple locking-free quasi-3D hyperbolic plate isogeometric method", *Compos. Part B-Eng.*, **120**, 182-196.
Mantari, J.L. and Monge, J.C. (2016), "Buckling, free vibration and bending analysis of functionally graded sandwich plates based on an optimized hyperbolic unified formulation", *Int. J. Mech. Sci.*, **119**, 170-186.
Mantari, J.L., Granados, E.V. and Soares, C.G. (2014), "Vibrational analysis of advanced composite plates resting on elastic foundation", *Compos. Part B-Eng.*, **66**, 407-419.
Nguyen, K., Thai, H.T. and Vo, T. (2015a), "A refined higher-order shear deformation theory for bending, vibration and buckling analysis of functionally graded sandwich plates", *Steel. Compos. Struct.*, *Int. J.*, **18**(1), 91-120.
Nguyen, N.T., Hui, D., Lee, J. and Nguyen-Xuan, H. (2015b), "An efficient computational approach for size-dependent analysis of functionally graded nanoplates", *Comput. Method. Appl. M.*, **297**, 191-218.
Nguyen, T.K., Nguyen, V.H., Chau-Dinh, T., Vo, T.P. and Nguyen-Xuan, H. (2016), "Static and vibration analysis of isotropic and functionally graded sandwich plates using an edge-based MITC3 finite elements", *Compos. Part B-Eng.*, **107**, 162-173.
Pagano, N.J. (1969), "Exact solutions for composite laminates in cylindrical bending", *J. Compos. Mater.*, **3**(3), 398-411.
Pagano, N.J. (1970), "Exact solutions for rectangular bidirectional composites and sandwich plates", *J. Compos. Mater.*, **4**(1), 20-34.
Qu, J., Zhang, Z., Luo, X., Li, B. and Wen, J. (2016), "A novel method to aging state recognition of viscoelastic sandwich structures", *Steel. Compos. Struct.*, *Int. J.*, **21**(6), 1183-1210.
Tebboune, W., Benrahou, K.H., Houari, M.S.A. and Tounsi, A. (2015), "Thermal buckling analysis of FG plates resting on elastic foundation based on an efficient and simple trigonometric shear deformation theory", *Steel. Compos. Struct.*, *Int. J.*, **18**(2), 443-465.
Thai, H.T. and Uy, B. (2013), "Levy solution for buckling analysis of functionally graded plates based on a refined plate theory", *Proceedings of the Institution of Mechanical Engineers*, *Part C*: *Journal of Mechanical Engineering Science*, **227**(12), 2649-2664.
Thai, C.H., Kulasegaram, S., Tran, L.V. and Nguyen-Xuan, H. (2014a), "Generalized shear deformation theory for functionally graded isotropic and sandwich plates based on isogeometric approach", *Comput. Struct.*, **141**, 94-112.
Thai, H.T., Vo, T., Bui, T. and Nguyen, T.K. (2014b), "A quasi-3D hyperbolic shear deformation theory for functionally graded plates", *Acta Mech.*, **225**(3), 951-964.
Viola, E., Rossetti, L. and Fantuzzi, N. (2012), "Numerical investigation of functionally graded cylindrical shells and panels using the generalized unconstrained third order theory coupled with the stress recovery", *Compos. Struct.*, **94**(12), 3736-3758.
Vu, T.V., Nguyen, N.H., Khosravifard, A., Hematiyan, M.R., Tanaka, S. and Bui, T.Q. (2017), "A simple FSDT-based meshfree method for analysis of functionally graded plates", *Eng. Anal. Bound. Elem.*, **79**, 1-12.
Wang, C.M., Ang, K.K., Yang, L. and Watanabe, E. (2000), "Free vibration of skew sandwich plates with laminated facings", *J. Sound Vib.*, **235**(2), 317-340.
Wu, P., Zhou, D., Liu, W., Lu, W. and Fang, H. (2017), "3-D exact solution of two-layer plate bonded by a viscoelastic interlayer with memory effect", *Compos. Struct.*, **164**, 291-303.
Xu, Y., Zhou, D. and Cheung, Y.K. (2008), "Elasticity solution of clamped-simply supported beams with variable thickness", *Appl. Math. Mech.-Eng.* **29**(3), 279-290.
Yan, C. and Song, X. (2016), "Effects of foam core density and face-sheet thickness on the mechanical properties of aluminum foam sandwich", *Steel. Compos. Struct.*, *Int. J.*, **21**(5), 1145-1156.
Yarasca, J., Mantari, J.L. and Arciniega, R.A. (2016), "Hermite–Lagrangian finite element formulation to study functionally graded sandwich beams", *Compos. Struct.*, **140**, 567-581.
Yu, T., Yin, S., Bui, T.Q., Liu, C. and Wattanasakulpong, N. (2017), "Buckling isogeometric analysis of functionally graded plates under combined thermal and mechanical loads", *Compos. Struct.*, **162**, 54-69.
Zenkour, A.M. (2007), "Benchmark trigonometric and 3-D elasticity solutions for an exponentially graded thick rectangular plate", *Arch. Appl. Mech.*, **77**(4), 197-214.

CC

Appendix

The details of the coefficients in Eqs. (11), (12) and (17) are given as follows

$$
\begin{aligned}
T_{mn}^1 &= \frac{r_{mn}{}^2 - t_{mn}{}^2 + k_i r_{mn} - \alpha_{mn}^2}{(r_{mn}{}^2 - t_{mn}{}^2 + k_i r_{mn} - \alpha_{mn}^2)^2 + (2r_{mn}t_{mn} + k_i t_{mn})^2},\\
T_{mn}^2 &= \frac{2r_{mn}t_{mn} + k_i r_{mn}}{(r_{mn}{}^2 - t_{mn}{}^2 + k_i r_{mn} - \alpha_{mn}^2)^2 + (2r_{mn}t_{mn} + k_i t_{mn})^2},\\
T_{mn}^3 &= \frac{s_{mn}{}^2 - t_{mn}{}^2 + k_i s_{mn} - \alpha_{mn}^2}{(s_{mn}{}^2 - t_{mn}{}^2 + k_i s_{mn} - \alpha_{mn}^2)^2 + (2s_{mn}t_{mn} + k_i t_{mn})^2},\\
T_{mn}^4 &= \frac{2s_{mn}t_{mn} + k_i t_{mn}}{(s_{mn}{}^2 - t_{mn}{}^2 + k_i s_{mn} - \alpha_{mn}^2)^2 + (2s_{mn}t_{mn} + k_i t_{mn})^2},
\end{aligned}
$$

$$
\begin{aligned}
R_{mn}^1 &= \frac{m\pi(\lambda_0^i + G_0^i)}{aG_0^i}[(r_{mn}^3 - 3r_{mn}t_{mn}^2)X_{mn}^3\\
&\quad + (r_{mn}^2 - t_{mn}^2)X_{mn}^2 + r_{mn}(X_{mn}^1 - 1) + X_{mn}^0] - \frac{k_i m\pi}{a},\\
R_{mn}^2 &= \frac{m\pi(\lambda_0^i + G_0^i)}{aG_0^i}[(3r_{mn}^2 t_{mn} - t_{mn}^3)X_{mn}^3\\
&\quad + 2r_{mn}t_{mn}X_{mn}^2 + t_{mn}(X_{mn}^1 - 1)],\\
R_{mn}^3 &= \frac{m\pi(\lambda_0^i + G_0^i)}{aG_0^i}[(s_{mn}^3 - 3s_{mn}t_{mn}^2)X_{mn}^3\\
&\quad + (s_{mn}^2 - t_{mn}^2)X_{mn}^2 + s_{mn}(X_{mn}^1 - 1) + X_{mn}^0] - \frac{k_i m\pi}{a},\\
R_{mn}^4 &= \frac{m\pi(\lambda_0^i + G_0^i)}{aG_0^i}[(3s_{mn}^2 t_{mn} - t_{mn}^3)X_{mn}^3\\
&\quad + 2s_{mn}t_{mn}X_{mn}^2 + t_{mn}(X_{mn}^1 - 1)],\\
R_{mn}^5 &= (r_{mn}^3 - 3r_{mn}t_{mn}^2)X_{mn}^3\\
&\quad + (r_{mn}^2 - t_{mn}^2)X_{mn}^2 + r_{mn}X_{mn}^1 + X_{mn}^0,\\
R_{mn}^6 &= (3r_{mn}^2 t_{mn} - t_{mn}^3)X_{mn}^3 + 2r_{mn}t_{mn}X_{mn}^2 + t_{mn}X_{mn}^1,\\
R_{mn}^7 &= (s_{mn}^3 - 3s_{mn}t_{mn}^2)X_{mn}^3\\
&\quad + (s_{mn}^2 - t_{mn}^2)X_{mn}^2 + s_{mn}X_{mn}^1 + X_{mn}^0,\\
R_{mn}^8 &= (3s_{mn}^2 t_{mn} - t_{mn}^3)X_{mn}^3 + 2s_{mn}t_{mn}X_{mn}^2 + t_{mn}X_{mn}^1,
\end{aligned}
\tag{A1}
$$

$$
p_{mn} = \frac{-k_{i+} + \sqrt{k_i^2 + 4\alpha_{mn}^2}}{2},
$$

$$
q_{mn} = \frac{-k_{i+} - \sqrt{k_i^2 + 4\alpha_{mn}^2}}{2},
$$

$$
\begin{aligned}
X_{mn}^0 &= \frac{k_i G_0^i \lambda_0^i \alpha_{mn}^2}{(\lambda_0^i + G_0^i)^2 \alpha_{mn}^2 + (k_i G_0^i)^2 \lambda_0^i / (\lambda_0^i + 2G_0^i)},\\
X_{mn}^1 &= \frac{k_i^2 (G_0^i)^2 + \lambda_0^i (\lambda_0^i + G_0^i)\alpha_{mn}^2}{(\lambda_0^i + G_0^i)^2 \alpha_{mn}^2 + (k_i G_0^i)^2 \lambda_0^i / (\lambda_0^i + 2G_0^i)},\\
X_{mn}^2 &= \frac{k_i G_0^i (\lambda_0^i + 2G_0^i)}{(\lambda_0^i + G_0^i)^2 \alpha_{mn}^2 + (k_i G_0^i)^2 \lambda_0^i / (\lambda_0^i + 2G_0^i)},\\
X_{mn}^3 &= \frac{G_0^i (\lambda_0^i + G_0^i)}{(\lambda_0^i + G_0^i)^2 \alpha_{mn}^2 + (k_i G_0^i)^2 \lambda_0^i / (\lambda_0^i + 2G_0^i)}.
\end{aligned}
\tag{A1}
$$

$$
\begin{aligned}
I_{mn}^1 &= \frac{m\pi}{a}(\lambda_0^i + 2G_0^i)(T_{mn}^1 R_{mn}^1 + T_{mn}^2 R_{mn}^2)\\
&\quad + \lambda_0^i [R_{mn}^5 - \frac{m\pi}{a}(T_{mn}^1 R_{mn}^1 + T_{mn}^2 R_{mn}^2)] - \lambda_0^i r_{mn},\\
I_{mn}^2 &= \frac{m\pi}{a}(\lambda_0^i + 2G_0^i)(T_{mn}^2 R_{mn}^1 - T_{mn}^1 R_{mn}^2)\\
&\quad - \lambda_0^i [R_{mn}^6 + \frac{m\pi}{a}(T_{mn}^2 R_{mn}^1 - T_{mn}^1 R_{mn}^2)] + \lambda_0^i t_{mn},\\
I_{mn}^3 &= \frac{m\pi}{a}(\lambda_0^i + 2G_0^i)(T_{mn}^3 R_{mn}^3 + T_{mn}^4 R_{mn}^4)\\
&\quad + \lambda_0^i [R_{mn}^7 - \frac{m\pi}{a}(T_{mn}^3 R_{mn}^3 + T_{mn}^4 R_{mn}^4)] - \lambda_0^i s_{mn},\\
I_{mn}^4 &= \frac{m\pi}{a}(\lambda_0^i + 2G_0^i)(T_{mn}^4 R_{mn}^3 - T_{mn}^3 R_{mn}^4)\\
&\quad - \lambda_0^i [R_{mn}^8 + \frac{m\pi}{a}(T_{mn}^4 R_{mn}^3 - T_{mn}^3 R_{mn}^4)] + \lambda_0^i t_{mn},
\end{aligned}
\tag{A2}
$$

$$
\begin{aligned}
J_{mn}^1 &= \\
&\quad \frac{m\pi}{a}\lambda_0^i (T_{mn}^1 R_{mn}^1 + T_{mn}^2 R_{mn}^2)\\
&\quad + (\lambda_0^i + 2G_0^i)[R_{mn}^5 - \frac{m\pi}{a}(T_{mn}^1 R_{mn}^1 + T_{mn}^2 R_{mn}^2)] - \lambda_0^i r_{mn},\\
J_{mn}^2 &= \\
&\quad \frac{m\pi}{a}\lambda_0^i (T_{mn}^2 R_{mn}^1 - T_{mn}^1 R_{mn}^2)\\
&\quad - (\lambda_0^i + 2G_0^i)[R_{mn}^6 + \frac{m\pi}{a}(T_{mn}^2 R_{mn}^1 - T_{mn}^1 R_{mn}^2)] + \lambda_0^i t_{mn},\\
J_{mn}^3 &= \\
&\quad \frac{m\pi}{a}\lambda_0^i (T_{mn}^3 R_{mn}^3 + T_{mn}^4 R_{mn}^4)\\
&\quad + (\lambda_0^i + 2G_0^i)[R_{mn}^7 - \frac{m\pi}{a}(T_{mn}^3 R_{mn}^3 + T_{mn}^4 R_{mn}^4)] - \lambda_0^i s_{mn},\\
J_{mn}^4 &= \\
&\quad \frac{m\pi}{a}\lambda_0^i (T_{mn}^4 R_{mn}^3 - T_{mn}^3 R_{mn}^4)\\
&\quad - (\lambda_0^i + 2G_0^i)[R_{mn}^8 + \frac{m\pi}{a}(T_{mn}^4 R_{mn}^3 - T_{mn}^3 R_{mn}^4)] + \lambda_0^i t_{mn},
\end{aligned}
\tag{A2}
$$

$$
\begin{aligned}
K_{mn}^1 &= (\lambda_0^i + 2G_0^i) r_{mn} - \lambda_0^i R_{mn}^5, \\
K_{mn}^2 &= -(\lambda_0^i + 2G_0^i) t_{mn} + \lambda_0^i R_{mn}^6, \\
K_{mn}^3 &= (\lambda_0^i + 2G_0^i) s_{mn} - \lambda_0^i R_{mn}^7, \\
K_{mn}^4 &= -(\lambda_0^i + 2G_0^i) t_{mn} + \lambda_0^i R_{mn}^8,
\end{aligned}
$$

$$
\begin{aligned}
L_{mn}^1 &= \frac{n\pi}{b} G_0^i (T_{mn}^1 R_{mn}^1 + T_{mn}^2 R_{mn}^2) \\
&\quad + \frac{mb}{na} G_0^i [R_{mn}^5 - \frac{m\pi}{a} (T_{mn}^1 R_{mn}^1 + T_{mn}^2 R_{mn}^2)], \\
L_{mn}^2 &= \frac{n\pi}{b} G_0^i (T_{mn}^2 R_{mn}^1 - T_{mn}^1 R_{mn}^2) \\
&\quad - \frac{mb}{na} G_0^i [R_{mn}^6 + \frac{m\pi}{a} (T_{mn}^2 R_{mn}^1 - T_{mn}^1 R_{mn}^2)], \\
L_{mn}^3 &= \frac{n\pi}{b} G_0^i (T_{mn}^3 R_{mn}^3 + T_{mn}^4 R_{mn}^4) \\
&\quad + \frac{mb}{na} G_0^i [R_{mn}^7 - \frac{m\pi}{a} (T_{mn}^3 R_{mn}^3 + T_{mn}^4 R_{mn}^4)], \\
L_{mn}^4 &= \frac{n\pi}{b} G_0^i (T_{mn}^4 R_{mn}^3 - T_{mn}^3 R_{mn}^4) \\
&\quad - \frac{mb}{na} G_0^i [R_{mn}^8 + \frac{m\pi}{a} (T_{mn}^4 R_{mn}^3 - T_{mn}^3 R_{mn}^4)],
\end{aligned}
$$

$$
\begin{aligned}
M_{mn}^1 &= G_0^i [(T_{mn}^1 R_{mn}^1 + T_{mn}^2 R_{mn}^2) r_{mn} \\
&\quad + (T_{mn}^2 R_{mn}^1 - T_{mn}^1 R_{mn}^2) t_{mn} + \frac{m\pi}{a}], \\
M_{mn}^2 &= G_0^i [(T_{mn}^2 R_{mn}^1 - T_{mn}^1 R_{mn}^2) r_{mn} \\
&\quad - (T_{mn}^1 R_{mn}^1 + T_{mn}^2 R_{mn}^2) t_{mn}], \\
M_{mn}^3 &= G_0^i [(T_{mn}^3 R_{mn}^3 + T_{mn}^4 R_{mn}^4) s_{mn} \\
&\quad + (T_{mn}^4 R_{mn}^3 - T_{mn}^3 R_{mn}^4) t_{mn} + \frac{m\pi}{a}], \\
M_{mn}^4 &= G_0^i [(T_{mn}^4 R_{mn}^3 - T_{mn}^3 R_{mn}^4) s_{mn} \\
&\quad - (T_{mn}^3 R_{mn}^3 + T_{mn}^4 R_{mn}^4) t_{mn}],
\end{aligned}
$$

$$
\begin{aligned}
N_{mn}^1 &= \frac{bG_0^i}{n\pi} [R_{mn}^5 r_{mn} - \frac{m\pi}{a} (T_{mn}^1 R_{mn}^1 + T_{mn}^2 R_{mn}^2) r_{mn} \\
&\quad - R_{mn}^6 t_{mn} - \frac{m\pi}{a} (T_{mn}^2 R_{mn}^1 - T_{mn}^1 R_{mn}^2) t_{mn} + \frac{n^2\pi^2}{b^2}], \\
N_{mn}^2 &= -\frac{bG_0^i}{n\pi} [R_{mn}^6 r_{mn} + \frac{m\pi}{a} (T_{mn}^2 R_{mn}^1 - T_{mn}^1 R_{mn}^2) r_{mn} \\
&\quad + R_{mn}^5 t_{mn} - \frac{m\pi}{a} (T_{mn}^1 R_{mn}^1 + T_{mn}^2 R_{mn}^2) t_{mn}], \\
N_{mn}^3 &= \frac{bG_0^i}{n\pi} [R_{mn}^7 s_{mn} - \frac{m\pi}{a} (T_{mn}^3 R_{mn}^3 + T_{mn}^4 R_{mn}^4) s_{mn} \\
&\quad - R_{mn}^8 t_{mn} - \frac{m\pi}{a} (T_{mn}^4 R_{mn}^3 - T_{mn}^3 R_{mn}^4) t_{mn} + \frac{n^2\pi^2}{b^2}], \\
N_{mn}^4 &= -\frac{bG_0^i}{n\pi} [R_{mn}^8 s_{mn} + \frac{m\pi}{a} (T_{mn}^4 R_{mn}^3 - T_{mn}^3 R_{mn}^4) s_{mn} \\
&\quad + R_{mn}^7 t_{mn} - \frac{m\pi}{a} (T_{mn}^3 R_{mn}^3 + T_{mn}^4 R_{mn}^4) t_{mn}].
\end{aligned}
\tag{A2}
$$

$$
\begin{aligned}
f_{mn}^{11}(z_i) &= [(T_{mn}^1 R_{mn}^1 + T_{mn}^2 R_{mn}^2) \cos(t_{mn} z_i) \\
&\quad + (T_{mn}^2 R_{mn}^1 - T_{mn}^1 R_{mn}^2) \sin(t_{mn} z_i)] e^{r_{mn} z_i} \\
f_{mn}^{12}(z_i) &= [(T_{mn}^1 R_{mn}^2 - T_{mn}^2 R_{mn}^1) \cos(t_{mn} z_i) \\
&\quad + (T_{mn}^2 R_{mn}^2 + T_{mn}^1 R_{mn}^1) \sin(t_{mn} z_i)] e^{r_{mn} z_i}, \\
f_{mn}^{13}(z_i) &= [(T_{mn}^3 R_{mn}^3 + T_{mn}^4 R_{mn}^4) \cos(t_{mn} z_i) \\
&\quad + (T_{mn}^4 R_{mn}^3 - T_{mn}^3 R_{mn}^4) \sin(t_{mn} z_i)] e^{s_{mn} z_i}, \\
f_{mn}^{14}(z_i) &= [(T_{mn}^3 R_{mn}^4 - T_{mn}^4 R_{mn}^3) \cos(t_{mn} z_i) \\
&\quad + (T_{mn}^4 R_{mn}^4 + T_{mn}^3 R_{mn}^3) \sin(t_{mn} z_i)] e^{s_{mn} z_i}, \\
f_{mn}^{15}(z_i) &= e^{p_{mn} z_i} E_{mn}^i, \quad f_{mn}^{16}(z_i) = e^{q_{mn} z_i} F_{mn}^i,
\end{aligned}
$$

$$
\begin{aligned}
f_{mn}^{21}(z_i) &= \\
&\{[R_{mn}^5 - \frac{m\pi}{a} (T_{mn}^1 R_{mn}^1 + T_{mn}^2 R_{mn}^2)] \cos(t_{mn} z_i) \\
&- [R_{mn}^6 + \frac{m\pi}{a} (T_{mn}^2 R_{mn}^1 - T_{mn}^1 R_{mn}^2)] \sin(t_{mn} z_i)\} \frac{b}{n\pi} e^{r_{mn} z_i}, \\
f_{mn}^{22}(z_i) &= \\
&\{[R_{mn}^6 - \frac{m\pi}{a} (T_{mn}^1 R_{mn}^2 - T_{mn}^2 R_{mn}^1)] \cos(t_{mn} z_i) \\
&+ [R_{mn}^5 - \frac{m\pi}{a} (T_{mn}^2 R_{mn}^2 + T_{mn}^1 R_{mn}^1)] \sin(t_{mn} z_i)\} \frac{b}{n\pi} e^{r_{mn} z_i}, \\
f_{mn}^{23}(z_i) &= \\
&\{[R_{mn}^7 - \frac{m\pi}{a} (T_{mn}^3 R_{mn}^3 + T_{mn}^4 R_{mn}^4)] \cos(t_{mn} z_i) \\
&- [R_{mn}^8 + \frac{m\pi}{a} (T_{mn}^4 R_{mn}^3 - T_{mn}^3 R_{mn}^4)] \sin(t_{mn} z_i)\} \frac{b}{n\pi} e^{s_{mn} z_i}, \\
f_{mn}^{24}(z_i) &= \\
&\{[R_{mn}^8 - \frac{m\pi}{a} (T_{mn}^3 R_{mn}^4 - T_{mn}^4 R_{mn}^3)] \cos(t_{mn} z_i) \\
&+ [R_{mn}^7 - \frac{m\pi}{a} (T_{mn}^4 R_{mn}^4 + T_{mn}^3 R_{mn}^3)] \sin(t_{mn} z_i)\} \frac{b}{n\pi} e^{s_{mn} z_i}, \\
f_{mn}^{25}(z_i) &= -\frac{bm}{an} e^{p_{mn} z_i}, \qquad f_{\mathrm{mn}}^{26}(z_i) = -\frac{bm}{an} e^{q_{mn} z_i},
\end{aligned}
\tag{A3}
$$

$$
\begin{aligned}
f_{mn}^{31}(z_i) &= e^{r_{mn} z_i} \cos(t_{mn} z_i), \quad f_{mn}^{32}(z_i) = e^{r_{mn} z_i} \sin(t_{mn} z_i), \\
f_{mn}^{33}(z_i) &= e^{s_{mn} z_i} \cos(t_{mn} z_i), \quad f_{mn}^{34}(z_i) = e^{s_{mn} z_i} \sin(t_{mn} z_i), \\
f_{mn}^{41}(z_i) &= [K_{mn}^1 \cos(t_{mn} z_i) + K_{mn}^2 \sin(t_{mn} z_i)] e^{(r_{mn} + k_i) z_i}, \\
f_{mn}^{42}(z_i) &= [K_{mn}^1 \sin(t_{mn} z_i) - K_{mn}^2 \cos(t_{mn} z_i)] e^{(r_{mn} + k_i) z_i}, \\
f_{mn}^{43}(z_i) &= [K_{mn}^3 \cos(t_{mn} z_i) + K_{mn}^4 \sin(t_{mn} z_i)] e^{(s_{mn} + k_i) z_i}, \\
f_{mn}^{44}(z_i) &= [K_{mn}^3 \sin(t_{mn} z_i) - K_{mn}^4 \cos(t_{mn} z_i)] e^{(s_{mn} + k_i) z_i},
\end{aligned}
$$

$$
\begin{aligned}
&f_{mn}^{51}(z_i)=[M_{mn}^{1}\cos(t_{mn}z_i)+M_{mn}^{2}\sin(t_{mn}z_i)]e^{(r_{mn}+k_i)z_i},\\
&f_{mn}^{52}(z_i)=[M_{mn}^{1}\sin(t_{mn}z_i)-M_{mn}^{2}\cos(t_{mn}z_i)]e^{(r_{mn}+k_i)z_i},\\
&f_{mn}^{53}(z_i)=[M_{mn}^{3}\cos(t_{mn}z_i)+M_{mn}^{4}\sin(t_{mn}z_i)]e^{(s_{mn}+k_i)z_i},\\
&f_{mn}^{54}(z_i)=[M_{mn}^{3}\sin(t_{mn}z_i)-M_{mn}^{4}\cos(t_{mn}z_i)]e^{(s_{mn}+k_i)z_i},\\
&f_{mn}^{55}(z_i)=G_0^i p_{mn}e^{(p_{mn}+k_i)z_i},\quad f_{mn}^{56}(z_i)=G_0^i q_{mn}e^{(q_{mn}+k_i)z_i},\\
&\\
&f_{mn}^{61}(z_i)=[N_{mn}^{1}\cos(t_{mn}z_i)+N_{mn}^{2}\sin(t_{mn}z_i)]e^{(r_{mn}+k_i)z_i},\\
&f_{mn}^{62}(z_i)=[N_{mn}^{1}\sin(t_{mn}z_i)-N_{mn}^{2}\cos(t_{mn}z_i)]e^{(r_{mn}+k_i)z_i},\\
&f_{mn}^{63}(z_i)=[N_{mn}^{3}\cos(t_{mn}z_i)+N_{mn}^{4}\sin(t_{mn}z_i)]e^{(s_{mn}+k_i)z_i},\\
&f_{mn}^{64}(z_i)=[N_{mn}^{3}\sin(t_{mn}z_i)-N_{mn}^{4}\cos(t_{mn}z_i)]e^{(s_{mn}+k_i)z_i},\\
&f_{mn}^{65}(z_i)=\frac{mbG_0^i}{na}p_{mn}e^{(p_{mn}+k_i)z_i},\\
&f_{mn}^{66}(z_i)=-\frac{mbG_0^i}{na}q_{mn}e^{(q_{mn}+k_i)z_i}.
\end{aligned}
\tag{A3}
$$